A finite element method to solve the compressible Navier-Stokes equations in 3D with mesh enrichment procedure

Samuel Boivin

INRIA

UNITE DE RECHERCHE
INRIA-ROCQUENCOURT

Institut National
de Recherche
en Informatique
et en Automatique

Domaine de Voluceau
Rocquencourt
B.P.105
78153 Le Chesnay Cedex
France
Tél. (1) 39 63 55 11

Rapports de Recherche

N° 1116

Programme 7
Calcul Scientifique,
Logiciels Numériques et Ingénierie Assistée

A FINITE ELEMENT METHOD TO SOLVE THE COMPRESSIBLE NAVIER-STOKES EQUATIONS IN 3D WITH MESH ENRICHMENT PROCEDURE

Sylvain BOIVIN

Novembre 1989

RR_1116

A FINITE ELEMENT METHOD TO SOLVE THE COMPRESSIBLE NAVIER-STOKES EQUATIONS IN 3D WITH MESH ENRICHMENT PROCEDURE.

Sylvain Boivin
(Dept. de mathématiques, Université Laval, Canada, G1K 7P4 and INRIA-Menusin, 78153 Le Chesnay, France)

Abstract:

A new computer code solving the compressible Navier-Stokes equations is described. The code solve the three-dimensional (3D), time-dependant equations using the finite element method based on the P1-P1isoP2 element. Actually the numerical stability is ensured by a simple artificial viscosity method which will be improved in a future version.

The results of numerical experiments for the flow around an ellipsoid will be presented in order to show the possibilities of the methods used.

Finally, we discuss an efficient mesh enrichment procedure which can be used in 2 or 3 dimension.

UNE METHODE NUMERIQUE DE TYPE ELEMENTS FINIS POUR RESOUDRE LES EQUATIONS DE NAVIER-STOKES COMPRESSIBLE EN 3D AVEC UNE PROCEDURE DE RAFFINEMENT LOCALE DU MAILLAGE.

Résumé:

Ce rapport décrit les techniques utilisées pour la mise au point d'un code de calcul permettant de simuler des écoulements compressibles. Les équations de Navier-Stokes compressibles, instationnaires, tridimensionnelles sont résolues via une approche différences finies en temps et éléments finis en espace utilisant l'élément P1-P1isoP2. Actuellement la stabilité du schéma est assurée par l'addition d'une simple viscosité artificielle qui sera améliorée dans une version ultérieure.

On présente des résultats numériques pour les écoulements autour d'un ellipsoide afin de démontrer les capacités de la méthode.

Finalement, nous présentons une méthode de raffinement locale de triangulations bi et tridimensionnelles.

Introduction.

In this report we consider the resolution of the compressible Navier-Stokes equations in three dimensional space using a finite element approach. We make use of the P1-P1isoP2 element, which proved to give good results in two dimension [BDGP][SB] and which gives a compatible approximation of the variables [BDGP]. As in the 2D case we use a P1 approximation for density and temperature variables on some grid, and also a P1 approximation for the velocity but on a finer grid. In 2D, the finer grid is obtained from the coarser by dividing each triangle in four by the meddle of the edges. In 3D, each tetraedra is cutted in eight tetraedras as shown in figure 1, bottom. The center of the element and is splitting in four tetraedra is shown in figure 2, top.

The numerical results are encouraging but more development are needed in order to obtain good result. In this way, we propose (in appendix) en efficient mesh enrichment procedure (2D and 3D), which enable us to obtain good results at low mach ($M \leq 2$) and low Reynolds number ($Re \leq 2000$). For the other cases, we hope a better stabilisation strategy (artificial viscosity) will give better results.

Numerical experiments are presented in order to show the possibilities of the methods discussed in this report.

1. Resolution of the Navier-Stokes equations in 3D.

Let $\Omega \in \mathbf{R}^3$, be the flow domain and Γ be its boundary. We now consider the following non-conservative non-dimensional form of the Navier-Stokes equations [SB]

$$\frac{\partial \rho}{\partial t} + u \cdot \nabla \rho + \rho \nabla \cdot u = 0 \tag{1.1}$$

$$\frac{\partial u}{\partial t} + (u \cdot \nabla)u + \frac{1}{\rho}\nabla p - \frac{1}{\rho}\nabla \cdot (\nu^* \sigma) = 0 \tag{1.2}$$

$$\frac{\partial T}{\partial t} + u \cdot \nabla T + \frac{p}{\rho}\nabla \cdot u - \nabla u : (\frac{\nu^*}{\rho}\sigma) - \frac{1}{\rho}\nabla \cdot (\kappa^* \nabla T) = 0 \tag{1.3}$$

in (1.1)-(1.3), we have normalized each variable by reference values denoted by the subscript r

(i) the density ρ by ρ_r
(ii) the velocity u by $|u_r|$
(iii) the internal energy e by $|u_r|^2$
(iv) the pressure p by $\rho_r |u_r|^2$
(v) the viscosity μ by μ_r
(vi) the temperature T by $|u_r|^2/C_v$
which imply $e = T$.

The pressure obeys the ideal gas law, the number γ and the functions σ, p, ν^*, κ^* are defined by:

$\bullet \sigma = \nabla u + \nabla u^t - \frac{2}{3}\nabla \cdot uI,$

$p = (\gamma - 1)\rho T,$

$\bullet \gamma = C_p/C_v$ is the ratio of specific heats ($\gamma \cong 1.4$ in air).

$\bullet \nu^* = \mu/Re_r$ is the total viscosity defined from the computed laminar viscosity divided by the reference Reynolds number $Re_r = \rho_r u_r L_r/\mu_r$.

$\bullet \kappa^* = \gamma/Re_r(\mu/Pr)$ is the total conductivity coefficient, also define from laminar viscosity.

We consider external flows around 3D geometries; the domain of computation is described in figure 2. Let Γ_∞ be a far-field boundary of the domain; we introduce

$$\Gamma_\infty^- = \{x | x \in \Gamma_\infty, u_\infty.n < 0\}, \qquad \Gamma_\infty^+ = \Gamma_\infty \backslash \Gamma_\infty^-$$

where u_∞ denotes the free stream velocity and n the unit vector of the outward normal to Γ.

We assume the flow to be uniform at infinity, and the corresponding variables to be normalized by the free stream values; then for example, we prescribe at infinity

$u = u_\infty = \begin{pmatrix} cos\alpha cos\beta \\ cos\alpha sin\beta \\ sin\alpha \end{pmatrix}$, α is the angle of attack, and β is the rolling angle.
$\rho = 1,$
$T = T_\infty = 1/[\gamma(\gamma - 1)M_\infty^2],$

where M_∞ denotes the free stream mach number.

The boundary conditions on the computational boundary Γ_∞ are:

on $\Gamma_\infty^- : u = u_\infty,\ T = T_\infty,\ \rho = 1,$
and on $\Gamma_\infty^+ : \nabla T \cdot n = 0\ ,\ \ n \cdot (\nabla u + \nabla u^t - \frac{2}{3}\nabla \cdot uI) = 0\ ,$
where n is the local normal on Γ_∞^+.

On the rigid boundary Γ_B, we shall use the following conditions:

$u = 0$ (no-slip condition),
$T = T_B = T_\infty(1 + (\gamma - 1)/2M_\infty^2)$ (free stream total temperature).

Finally, since steady solutions are sought through time dependent equations, initial conditions have to be added; we shall take

$\rho(x,0) = \rho_o(x), \quad u(x,0) = u_o(x), \quad T(x,0) = T_o(x).$

Solving the compressible Navier-Stokes equations is a difficult task. Most of the existing numerical solution methods are based on finite differences techniques, for both space and time discretizations. Following the work of Bristeau et al. [BGMPR][BDGP] and Boivin [SB], we will consider a method based on finite element techniques for space discretization while using finite differences in time.

Let the time derivatives be discretized using a classical implicit Euler finite differences formula, then at each time step, we solve the following non-linear system of variational equations

$$\alpha(\rho - \hat{\rho}, N) + (u \cdot \nabla\rho, N) + (\rho\nabla \cdot u, N) = 0 \tag{1.4}$$

$$\alpha(u - \hat{u}, M) + ((u \cdot \nabla)u, M) + (\frac{1}{\rho}\nabla p, M) + (\frac{\hat{\nu}^*}{\rho}\sigma, \nabla M) = 0 \tag{1.5}$$

$$\alpha(T - \hat{T}, K) + (u \cdot \nabla T, K) + (\frac{p}{\rho}\nabla \cdot u, K) - (\nabla u : (\frac{\hat{\nu}^*}{\rho}\sigma), K) + (\frac{\hat{\kappa}^*}{\rho}\nabla T, \nabla K) = 0 \tag{1.6}$$

where the solution is looked for in V x W x Z,

$$V = \{\rho \in H^1(\Omega) | \rho_{|\Gamma_\infty^-} = 1\}$$

$$W = \{u \in (H^1(\Omega))^3 | u_{|\Gamma_\infty^-} = u_\infty, u_{|\Gamma_B} = 0\}$$

$$Z = \{T \in H^1(\Omega) | T_{|\Gamma_\infty^-} = T_\infty, T_{|\Gamma_B} = T_B\}$$

although there is no existence theorem for this problem. We look for a triple $(\rho, u, T) \in V$ x W x Z such that (1.4)-(1.6) is verify for all triple of test functions $(N, M, K) \in Y(\Omega)$ x $(X(\Omega))^3$ x $X(\Omega)$. Where the spaces $X(\Omega)$, $Y(\Omega)$ are defined by

$$X(\Omega) = \{x \in H^1(\Omega) | x_{|\Gamma_\infty^-} = 0\}$$

$$Y(\Omega) = \{x \in H^1(\Omega) | x_{|\Gamma_\infty^-} = 0\}$$

Remark 1: (,) denotes the scalar product in $L^2(\Omega)$.
Remark 2: The natural boundary condition already defined were introduced by setting the boundary integrals appearing from the integration by part to zero.
Remark 3: The p term of equation (1.5) is integrated in the form

$$\frac{1}{\rho}\nabla p = (\gamma - 1)\nabla T + (\gamma - 1)\frac{T}{\rho}\nabla\rho.$$

We do not integrate by part the pressure term of the momentum equation because we cannot set $p + \sigma_{nn} = 0$ on the boundary (doing so would perturbate the solution) and we prefer to avoid the computation of boundary integrals.

To approximate (1.4)-(1.6), by the finite element method, we must divide Ω into small elements (tetraedra) and replace all the functions by their interpolate ρ_h, u_h, T_h. Interpolates are defined inside the elements from their values at the nodes of the elements by an interpolation formula.

To insure the compatibility between the approximation of density, temperature and velocity (see [BDGP]) we use the P1-P1isoP2 element of figure 1 and we define

$$V_h = \{\rho_h \in V | \rho_h \in C^o(\Omega), \forall \mathrm{T} \in \mathrm{T_h}, \rho_{\mathrm{h|T}} \in \mathrm{P^1(T)}\} \subset \mathrm{V}$$

$$W_h = \{u_h \in W | u_h \in (C^o(\Omega))^3, \forall \mathrm{T} \in \mathrm{T_{h/2}}, \mathrm{u_{h|T}} \in \mathrm{P^1(T)}\} \subset \mathrm{W}$$

$$Z_h = \{T_h \in Z | T_h \in C^o(\Omega), \forall \mathrm{T} \in \mathrm{T_h}, \mathrm{T_{h|T}} \in \mathrm{P^1(T)}\} \subset \mathrm{Z}$$

where $P^1(\mathrm{T}) = \{$ set of polynomials of degree ≤ 1 on T$\}$ and T denote an element of the P1 mesh $\mathrm{T_h}$ or the P1isoP2 mesh $\mathrm{T_{h/2}}$.

Restricted to these finite dimensional spaces, equations (1.4)-(1.6) lead to the non-linear problem:

$$\text{Find } (\rho_h, u_h, T_h) \text{ in } (V_h \text{ x } W_h \text{ x } Z_h) \text{ solution of } F_h(\rho_h, u_h, T_h) = 0\ , \tag{1.7}$$

F_h being the discrete version of the system (1.4)-(1.6).

We now consider iteration schemes for solving the nonlinear system $F_h(s) = 0$, where $s = (\rho_h, u_h, T_h)$.

Newton's method applied to this system results in the iteration

1. Set s^o an initial guess
2. For n = 0,1,2,... until convergence do:
   2.1 Solve $J(s^n)\delta^n = -F_h(s^n)$,
   2.2 Set $s^{n+1} = s^n + \delta^n$,

(1.8)

where $J(s^n) = F'(s^n)$ is the system Jacobian. For large problems, iterative methods are frequently used to solve (1.8) only approximately, giving rise to methods which can be viewed as inexact Newton methods. The particular method we use is the Generalized Minimum Residual Method (GMRES) due to Saad and Schultz [SS]. This method has the virtue of requiring virtually no matrix storage and requires only the action of the Jacobian matrix J times a vector r, and not J explicitly. In the setting of nonlinear equations, this action is approximated by a difference quotient of the form

$$J(s)r \cong \frac{F_h(s + br) - F_h(s)}{b}$$

where s is the current approximation of a root of (1.7) and b is a scalar. For details of the algorithm, see Saad-Schultz [SS] and also Bristeau et al. [BGMPR] for a clear setting of this algorithm within the context of the conjugate gradient methods.

To insure numerical stability an artificial viscosity is added to each equation. Actually, this term is a Laplacian with a coefficient proportional to the local mesh size ($\alpha \|u\| h$). A future version with a better stabilization strategy is under development.

2. Two and three dimensional mesh enrichment procedure.

Many numericians are now concerned by the problem of enrichment and adaptation of meshes. The reason is clear, these techniques may enable us to obtain optimal results for a given number of degres of freedom. Some method are now avaiable, [P][BGMPR][CP], but in most of them two problems remain; the definition of optimal result for a given number of degres of freedom and the complexity of the algorithms.

We propose an efficient mesh enrichment algorithm, which is easily implemented in 2D and also in 3D.

I- Two dimensional case.

We suppose given a triangulation (T_h) and a criteria ($0 \leq c(T) \leq 1$) defined for each triangle. Our goal is to subdivide each triangle for which the criteria is between two given values ($cmin$ and $cmax$). We define

$$Q = \{ T \in T_h \mid cmin \leq c(T) \leq cmax \}$$

The basic step of the method is to divide each triangle of a set $H(Q)$, dependent of Q, in three triangles by the addition of a node at the barycenter of the father triangle, figure 6 top. The set $H(Q)$ is defined through the following steps (we denote $v(T)$ the set of triangles having a common edge with T)

1) each triangle of T_h for which 2 or 3 members of $v(T)$ are in Q are added to the set Q, we also denote by Q this new set,

2) each triangle of Q for which 0 or 1 members of $v(T)$ are in Q are eliminated from this set.

After dividing each triangle of the set $H(Q)$ the following smooting process is applied

1) each edge of T_h between two newly divided triangle is flipped, figure 6 middle,

2) each newly divided triangle with an edge on a boundary is cut again in two triangles by the addition of a node on the boundary, figure 6 bottom.

II- Three dimensional case.

The construction of the set $H(Q)$ is the same as in case I. The division step is similar; a node is added at the barycenter of each tetraedra of $H(Q)$ and the tetraedra is splitted

in four, figure 7 top. But the smooting step is more complex and given by (here $v(T)$ is the set of tetraedras of T_h having a common face with T)

1) each face (bcd) between two newly divided tetraedra (abcd) and (bcde) is eliminated by the replacement of these two tetraedras by three tetraedras (aebc) (aecd) (aebd), figure 7 middle.

2) each face of $H(Q)$ on a boundary is splitted in three by the addition of a node at its barycenter creating three additional tetraedras, figure 7 bottom.

3. Numerical experiments.

Computation were made for some flow conditions around an ellipsoid in order to show the potential of the method we propose. The mesh contains 20671 P1-P1isoP2 elements for 4069 P1 nodes and 29767 P1isoP2 nodes for a total of 97439 degres of freedom. It took 90 time step to reach a steady state (we stopped when the correction in infinity norm was lower then 10^{-4}) and 26 hours of computation on an Apollo DN10000.

Figure 3 show the skin mesh of the ellipsoid and also of the boundary edge while figure 4 show the trace of the mesh in the XY plane. Figure 5 show the isomach contours for a computation at mach=2.0 and Reynolds=1000.

Actually a finer grid would be necessary in order to capture the choc wave and the boundary layer.

We present an example of the use of the mesh enrichment procedure in 2D (figures 8 to 12) and one example in 3D (figures 13 to 17) in the context of Navier-Stokes calculation around a body [SB].

Figures 8 and 9 shows the initial mesh and the mach number field of the initial 2D supersonic Navier-Stokes calculation. Figures 10 and 11 shows the enrichments of triangles for which the mach gradient is greater then 10 % of its maximum value. In the second case a supplementary smooting process were applied: each node is moved at the barycenter of the cell formed by the triangles containing this node. Figure 12 show the mach number field obtained after few more steps of calculations from the initial solution reinterpolated on the mesh of figure 11.

Figures 13 and 14 shows the trace of the initial mesh in the XY plane and the mach number field (on the same plane) of the initial 3D supersonic Navier-Stokes calculation. As we are interested to capture the choc, we enrich the mesh in the area captured by the criteria of figure 15, computed from the initial solution. The trace of the new mesh in the XY plane is showed in figure 16 while the mach number field obtained after few more step of calculations, starting from the initial solution interpolated on this mesh, is showed in figure 17. Actually, comparison of figures 13 and 16 give a good idea of the enrichment done throught the process, but it don't give any information about the quality of the mesh.

4. Conclusions.

We have briefly discussed here a finite element method to solve the three-dimensional compressible Navier-Stokes equations written in non conservative form. In it's actual setting the method is rather costly in computer time and restricted to low Mach and Reynolds numbers flows. We can hope from the first results that, for higher Mach and Reynolds numbers, giving a better stabilization method (artificial viscosity), we will obtain accurate solutions.

Appendix 1: Integration.

The nonlinear discrete system of equations to be solved follows from the consideration of the variational system (1.4)-(1.6) on proper finite dimensional spaces. Exact definitions of these spaces and the corresponding test spaces follow from the choice of the finite element. Now remains the problem of the evaluation of the various term, that is, the choice of an integration strategy. Exact integration will be use for first order terms but approximation will be made for higher order terms.

The basic formula for the integration is the Simpson's formula

$$\int_T w dx = \frac{-|T|}{20} \sum_{i=1}^{4} w(M_{iT}) + \frac{|T|}{5} \sum_{i=1}^{6} w(m_{iT}), \qquad \forall w \in P_2,$$

where M_{iT} and m_{iT} are the nodes and midnodes of the tetraedra T. Thus, the integral of the product of $f \in P_1$ by $g \in P_1$ on the same tetraedra will be given by

$$\int_T fg dx = \frac{|T|}{20} \left[\left(\sum_{i=1}^{4} f(M_{iT}) g(M_{iT}) \right) + \left(\sum_{i=1}^{4} f(M_{iT}) \right) \left(\sum_{i=1}^{4} g(M_{iT}) \right) \right], \ \forall f, g \in P_1,$$

where M_{iT} are the nodes of T. For simplicity, these formulas are also used for higher order terms.

Acknowledgments.

This work is partly supported by a contract from Avions Marcel Dassault - Bréget Aviation and was carried out during the author's stay at the Institut National de Recherche en Informatique et en Automatique (INRIA) in France.

I would like to thank specially O. Pironneau, E. Saltel and A. Golgolab for their help in creating 3D meshes and for fruitful discussions.

References.

S. Boivin [SB] : A numerical method for solving the compressible Navier-Stokes equations, IMPACT of Computing in Science and Engineering, Academic Press Boston, 1, (1989).

M.O. Bristeau, L. Dutto, R. Glowinski, J. Périaux [BDGP] : Compressible viscous flow calculations using compatible finite element approximations, Proc. of the 7th Int. Conf. on Finite Element Meth. in Flow Problems, Huntsville, Alabama, (1989).

M.O. Bristeau, R. Glowinski, J. Périaux [BGP] : Numerical methods for the Navier-Stokes equations. Application to the simulation of compressible and incompressible viscous flows, Computer Physics Reports 6, (1987).

M.O. Bristeau, R. Glowinski, B. Mantel, J. Périaux, G. Rogé [BGMPR] : Adaptative finite element methods for three dimensional compressible viscous flow simulation in aerospace engineering, in: 11th Inter. Conf. on Numer. Meth. in Fluid Dynamics, Springer-Verlag (to be published) (1988).

B. Palmerio [P] : Self-adaptive F.E.M. algorithms for the Euler equations, INRIA Research Report no.338 (1984).

O. Pironneau, J. Rappaz [PR] : Numerical analysis for the compressible viscous adiabatic stationary flows, IMPACT of Computing in Science and Engineering, Academic Press Boston, 1, (1989).

C. Pouletty [CP] : Génération et optimisation de maillages en éléments finis. Application à la résolution de quelques équations en mécanique des fluides. Thèse de Docteur Ingénieur, Ecole Centrale des Arts et Manufactures, (1985).

Y. Saad and M.H. Schultz [SS] : GMRES: A generalized minimal residual algorithm for solving nonsymmetric linear systems, SIAM J. Sci. Stat. Comp., 7 (1986).

In 2D

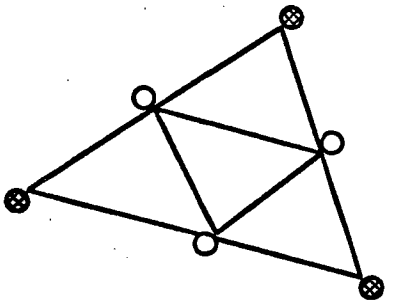

⊗ velocity, density and temperature d.o.f.

O velocity d.o.f. only

In 3D

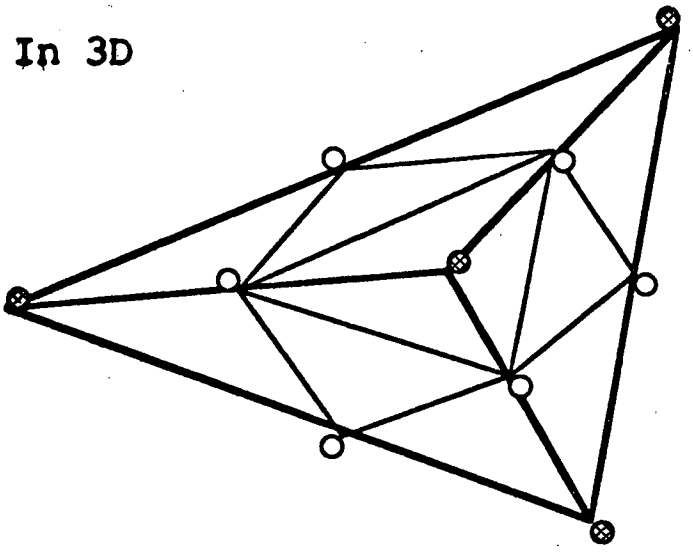

⊗ velocity, density and temperature d.o.f.

O velocity d.o.f. only

Figure 1. P1-P1isoP2 element in 2D and in 3D.

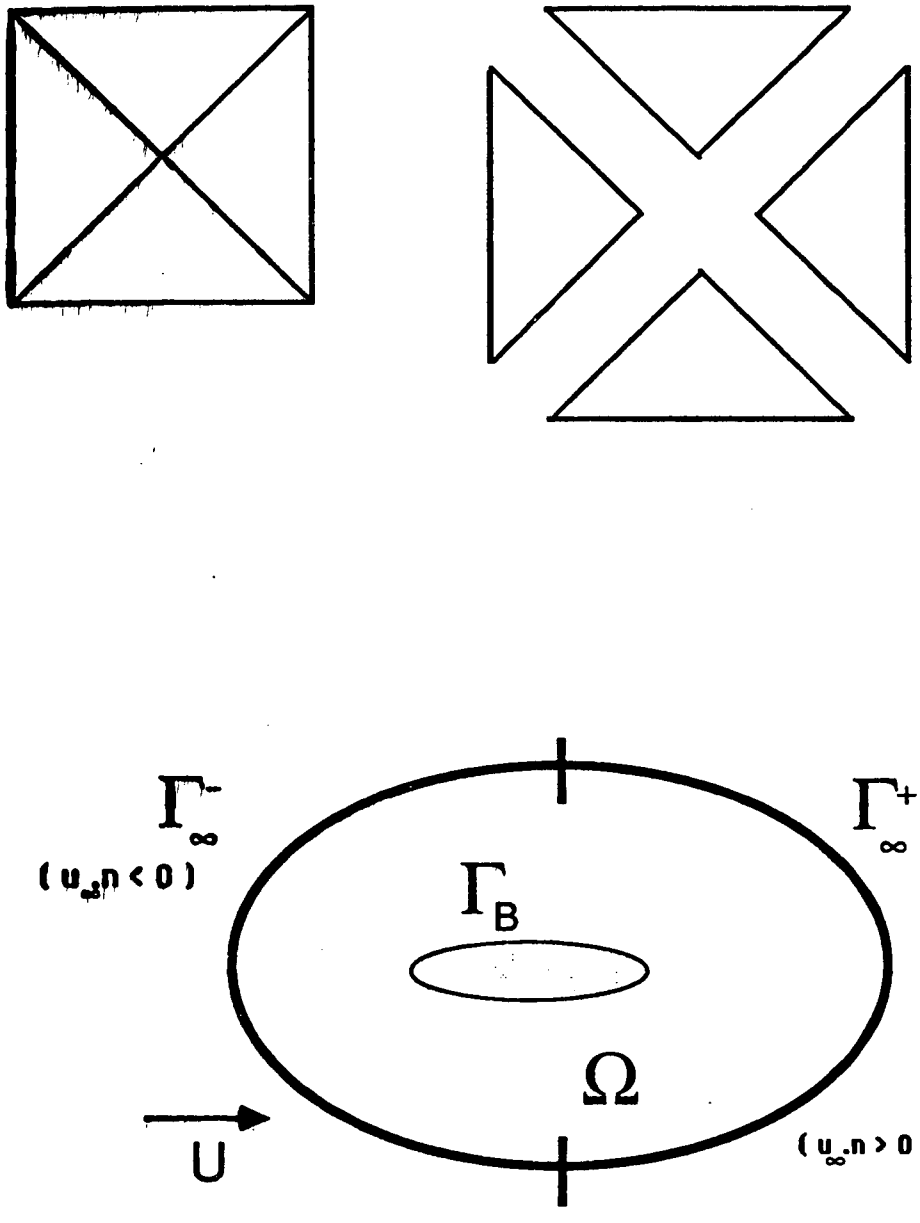

Figure 2,
Top: Splitting of the center part of the P1-P1isoP2 in 3D.
Bottom: Computational domain in 2D. Cut along the XZ plane of the 3D computational domain.

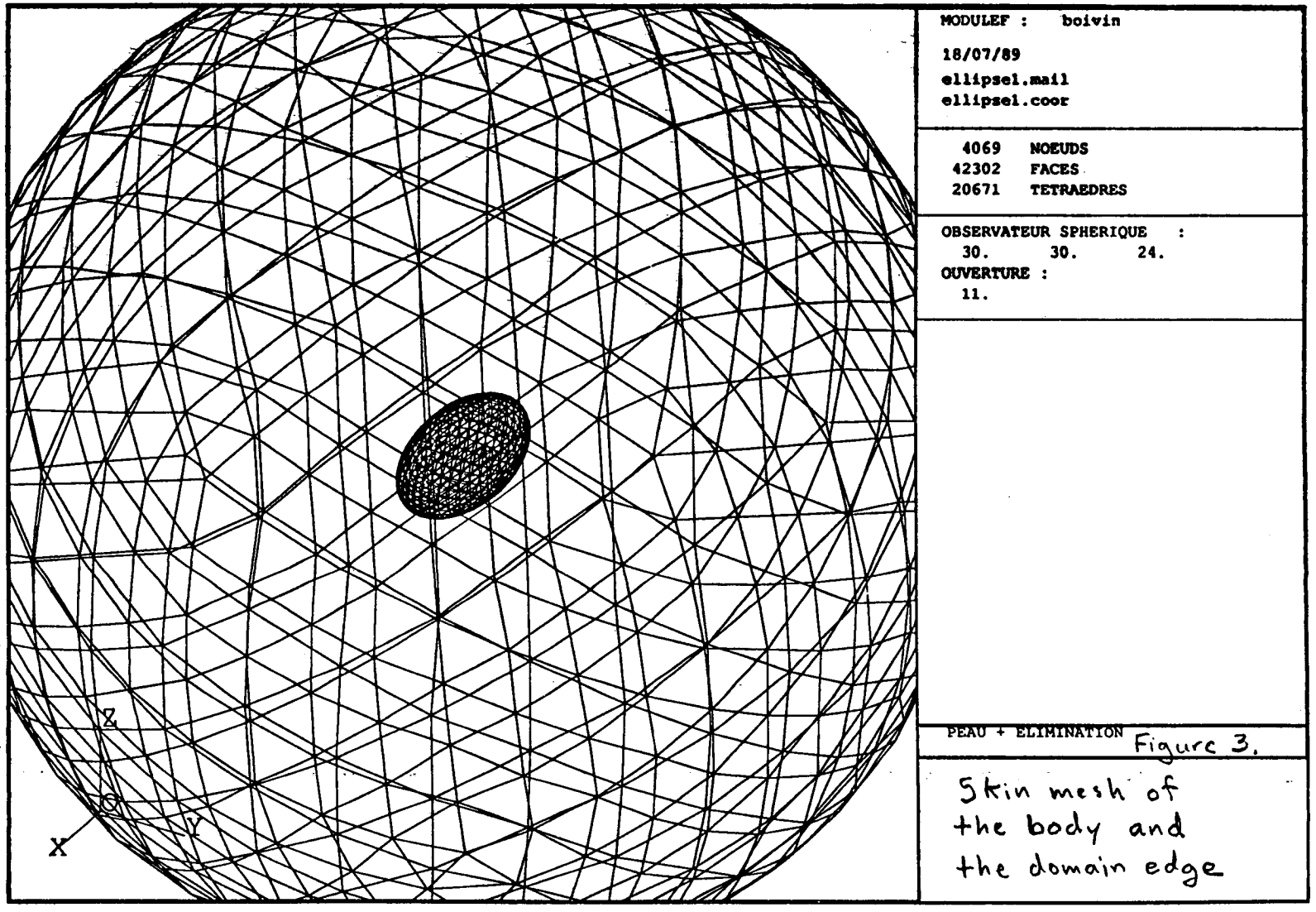

MODULEF : boivin

18/07/89
ellipsel.mail
ellipsel.coor

4069 NOEUDS
42302 FACES
20671 TETRAEDRES

OBSERVATEUR SPHERIQUE :
30. 30. 24.
OUVERTURE :
11.

PEAU + ELIMINATION

Figure 3.

Skin mesh of the body and the domain edge

le 18:07:1989 a 15h 07mn. Utilisateur: boivin Dessin 1

Trace of the 3D mesh in the XY plane

Figure 4.

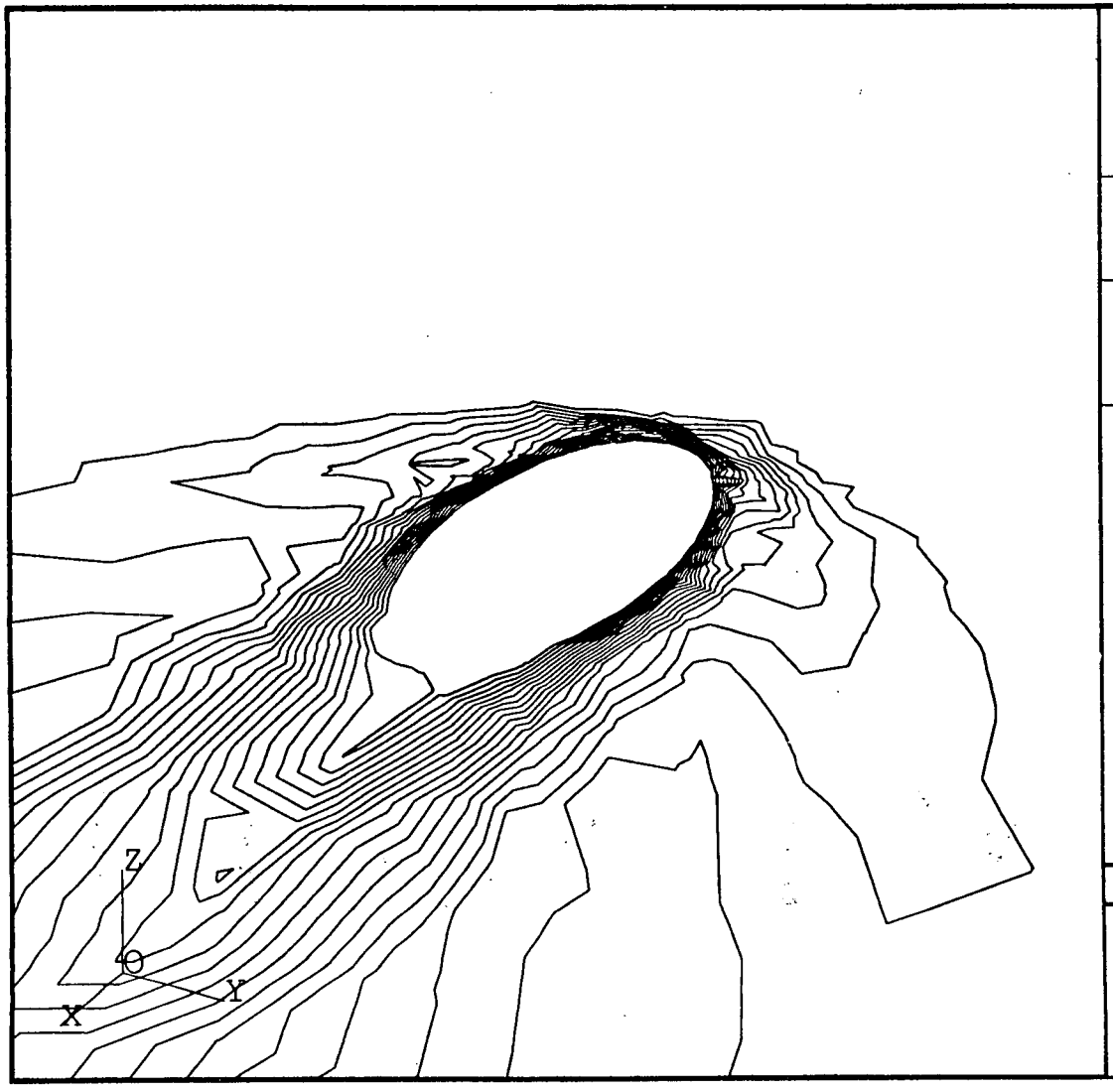

MODULEF : boivin

11/08/89
ellipse.mail
ellipse.coor
solu.b

4069 NOEUDS
42302 FACES
20671 TETRAEDRES

OBSERVATEUR SPHERIQUE :
30. 30. 12.
OUVERTURE :
11.

ISOVALEURS : 20
INCONNUE : 1 MNEMO :VN

20	2.117
19	2.006
18	1.894
17	1.783
16	1.671
15	1.560
14	1.449
13	1.337
12	1.226
11	1.114
10	1.003
9	0.8915
8	0.7800
7	0.6686
6	0.5572
5	0.4457
4	0.3343
3	0.2229
2	0.1114
1	0.0000

Iso M

PEAU VUE + ELIMINATION Figure 5

$M_\infty = 2$

$Re_\infty = 2000$

Version 2.04 de Portran.sd LMLL/A le 11:08:1989 a 14h 43mn. Utilisateur: boivin Dessin 1

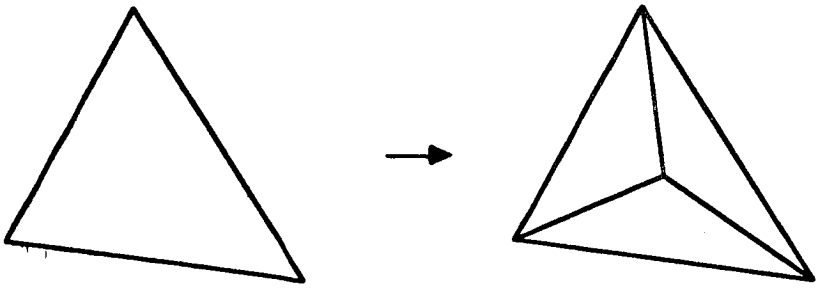

Enrichement by the addition of one node.

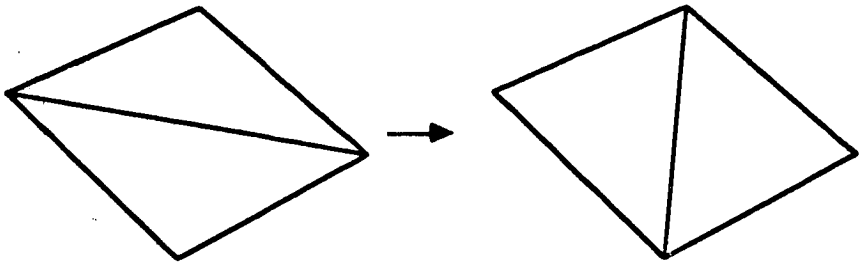

Edge flipping between two triangles.

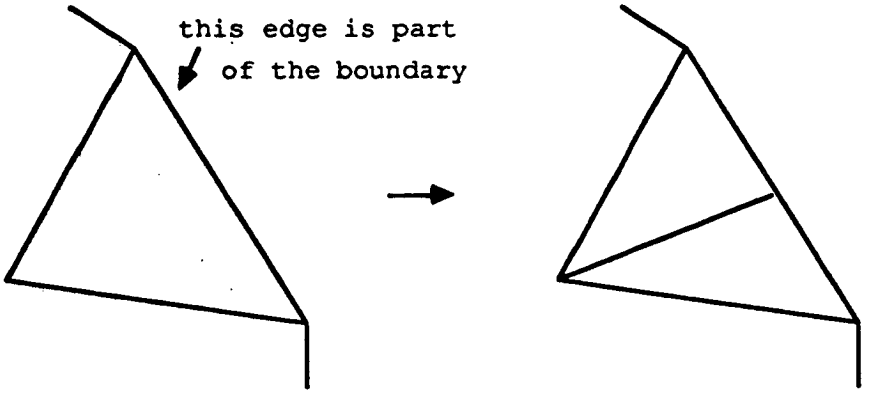

Secondary enrichment near a boundary.

Figure 6. Example of the 2D division and smooting.

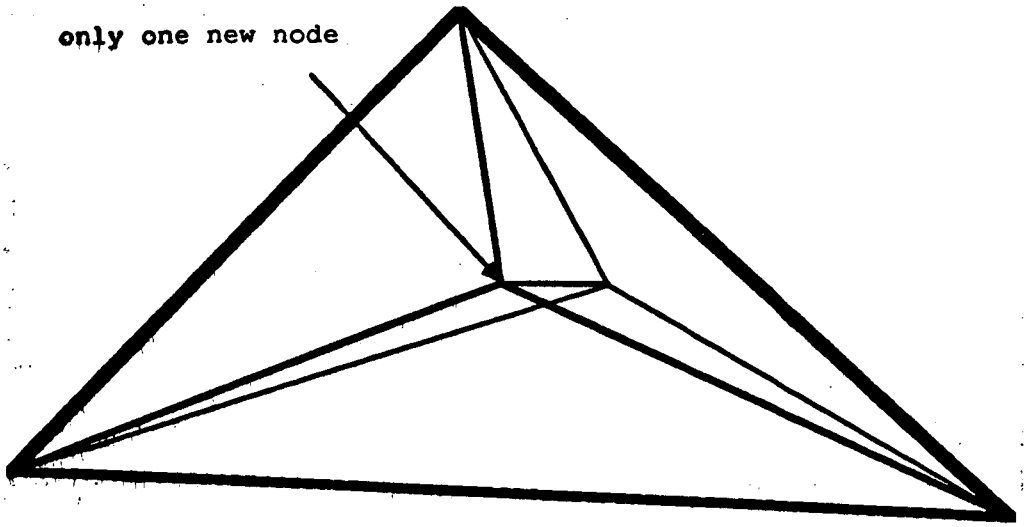

Enrichment by the addition of one node.

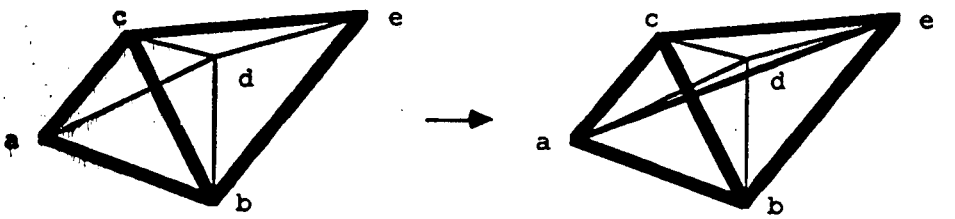

2->3 smooting process

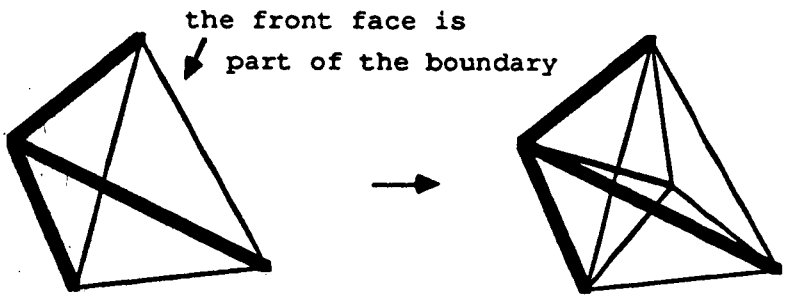

Secondary enrichment near a boundary.

Figure 7. Example of the 3D division and smooting.

Notice: finer lines are in front.

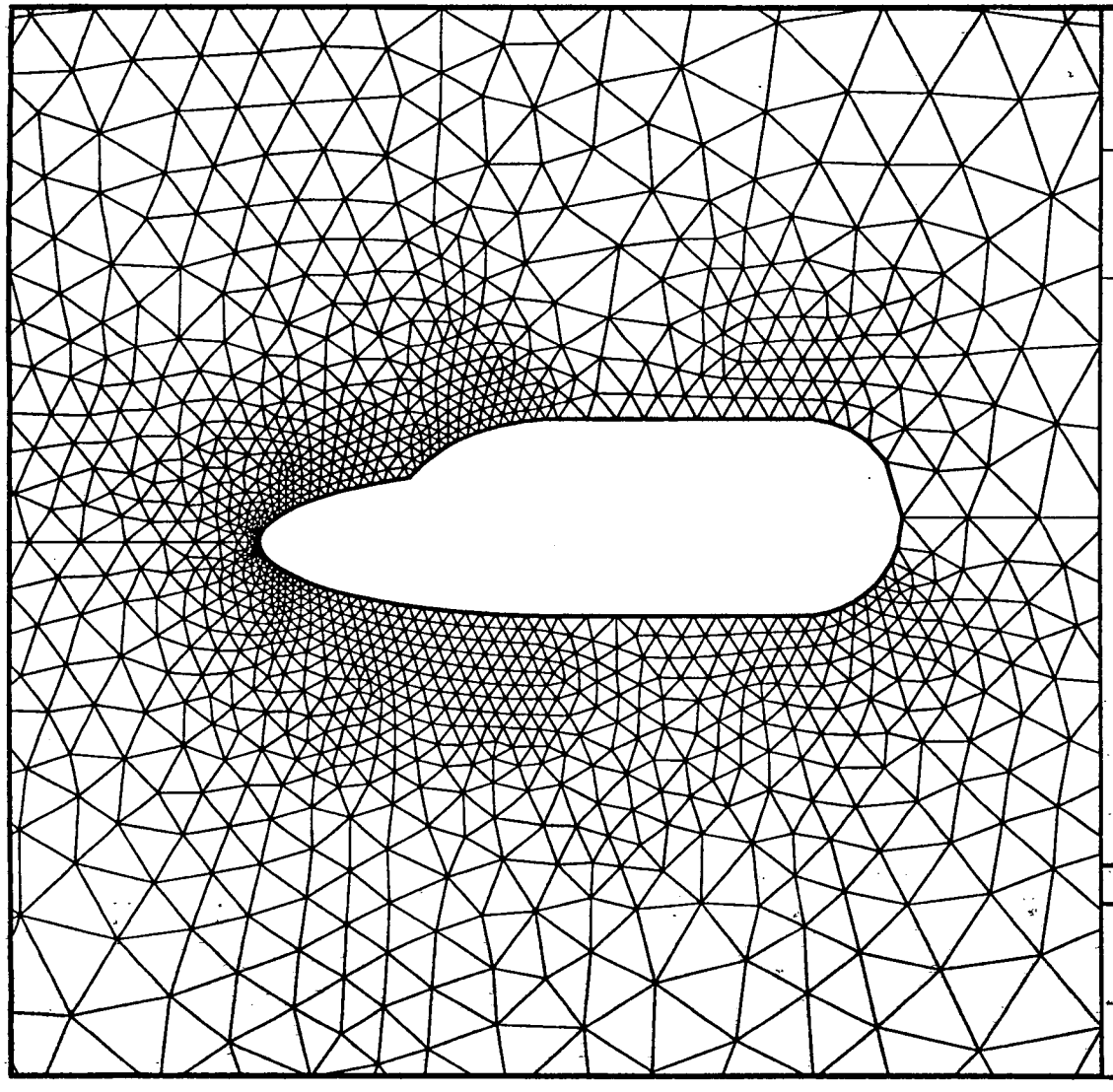

MODULEF : boivin

07/07/89
n.mail
n.coor

1883 POINTS
1883 NOEUDS
3606 ELEMENTS
3606 TRIANGLES

Figure 8.

Basic mesh

Version 2.04 de Perron 3d I.N.R.I.A. le 07:07:1989 a 15h 44mn. Utilisateur: boivin Dessin 1

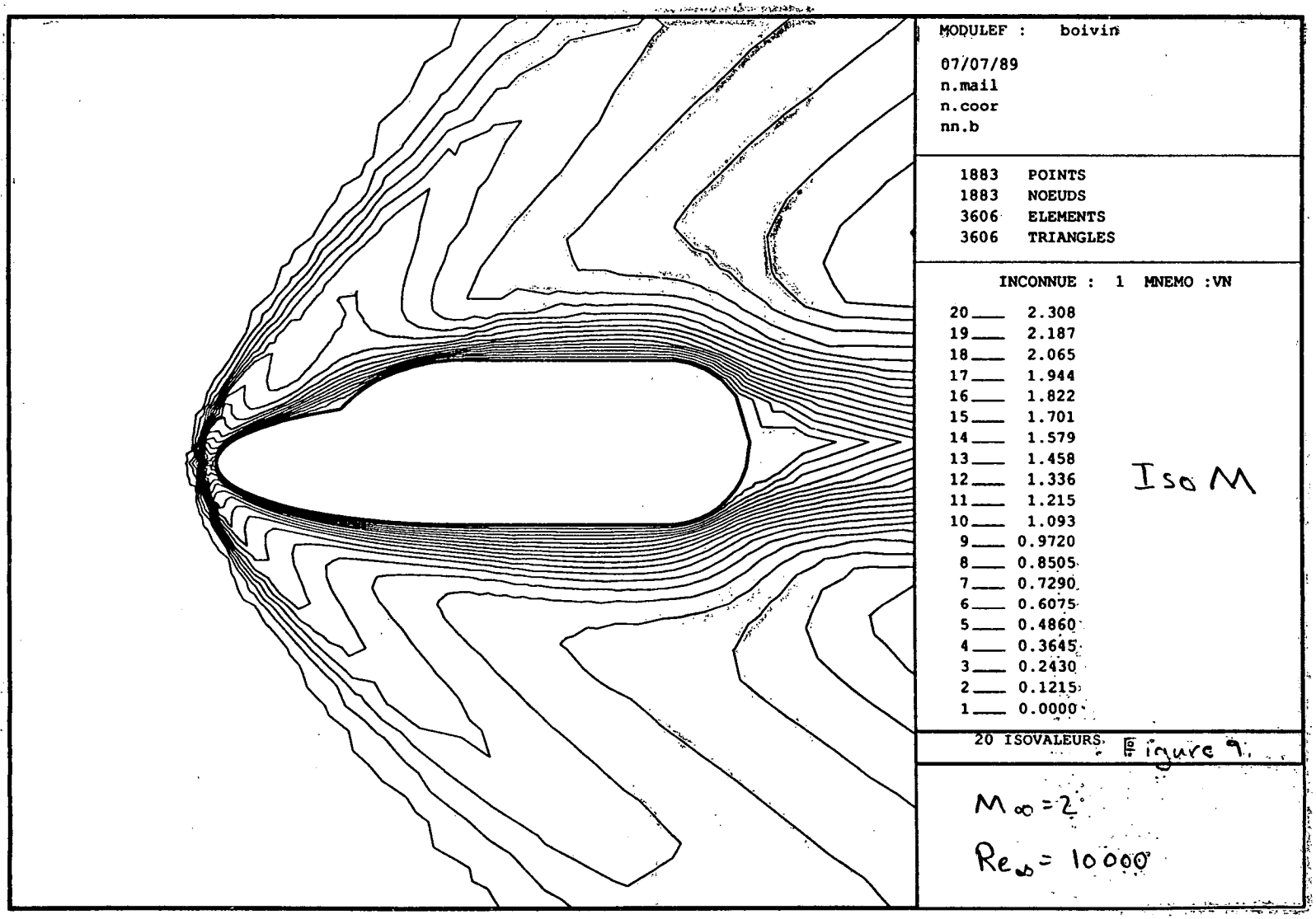

MODULEF : boivin

07/07/89
n.mail
n.coor
nn.b

1883 POINTS
1883 NOEUDS
3606 ELEMENTS
3606 TRIANGLES

INCONNUE : 1 MNEMO :VN

20	2.308
19	2.187
18	2.065
17	1.944
16	1.822
15	1.701
14	1.579
13	1.458
12	1.336
11	1.215
10	1.093
9	0.9720
8	0.8505
7	0.7290
6	0.6075
5	0.4860
4	0.3645
3	0.2430
2	0.1215
1	0.0000

Iso M

20 ISOVALEURS

Figure 9.

$M_\infty = 2$

$Re_b = 10000$

Version 2.04 de Perron 94 LN.R.L.A. le 07:07:1989 a 15h 51mn. Utilisateur: boivin Dessin 1

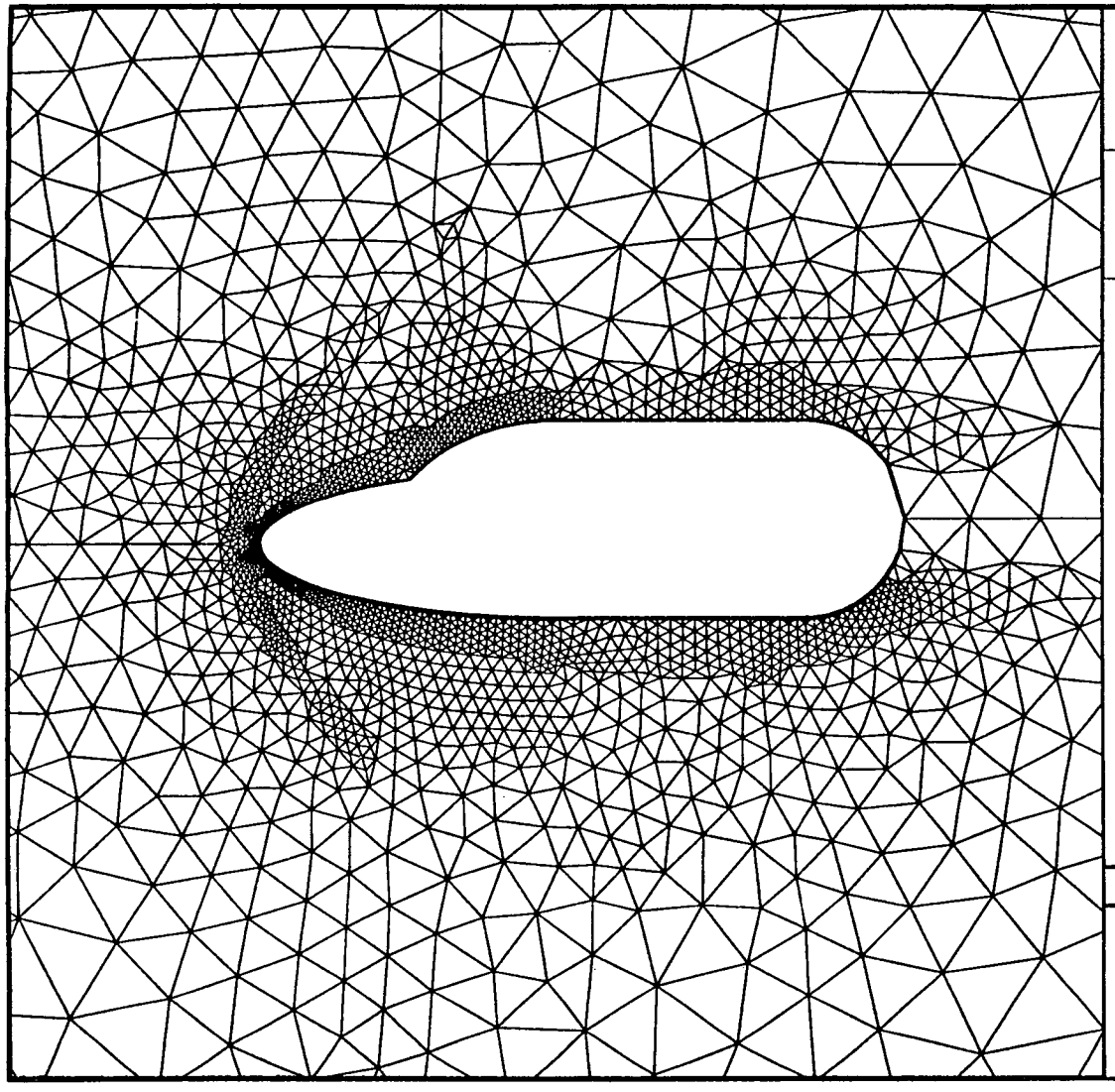

MODULEF : boivin

10/07/89
nn.m
nn.c

2708 POINTS
2708 NOEUDS
5162 ELEMENTS
5162 TRIANGLES

Figure 10.

Refined mesh
Criteria : $|\nabla M|$

Version 2.04 de Perform 3d LNERLA *le 10:07:1989 a 10h 20mn. Utilisateur: boivin Dessin 1*

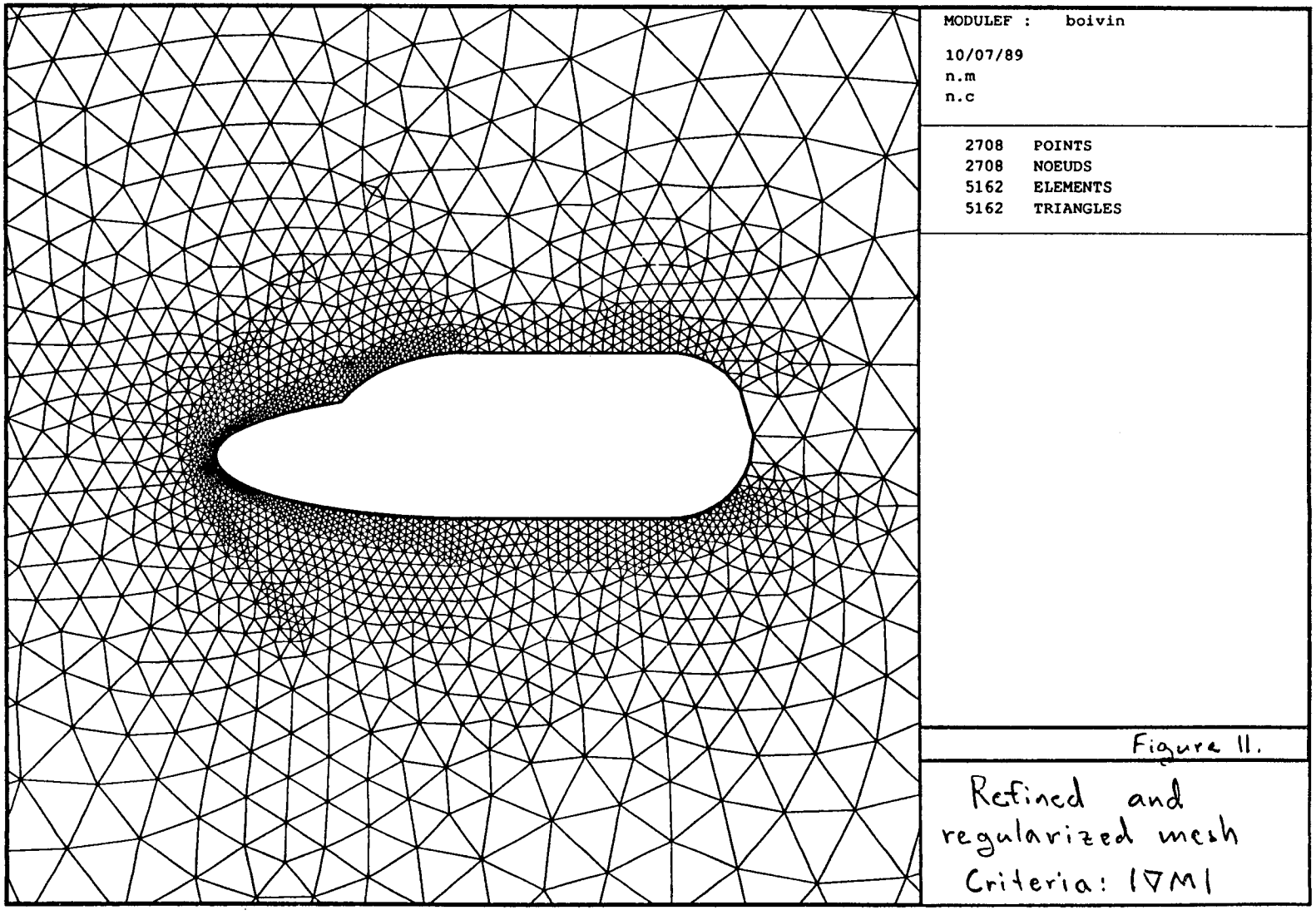

Figure 11.

Refined and regularized mesh
Criteria: $|\nabla M|$

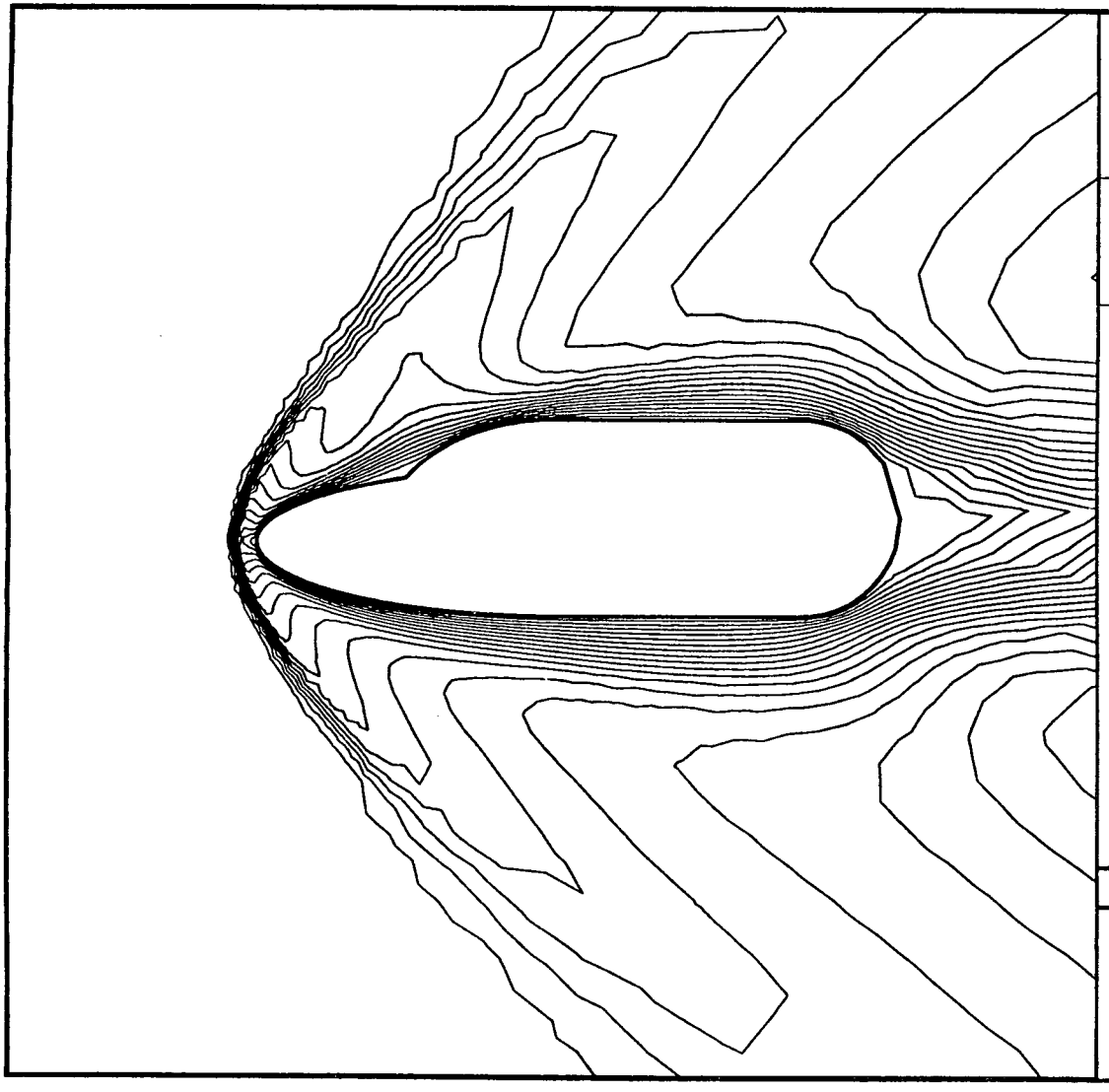

MODULEF : boivin

13/07/89
nc.m
nc.c
sm.b

2708 POINTS
2708 NOEUDS
5162 ELEMENTS
5162 TRIANGLES

INCONNUE : 1 MNEMO :VN

20 ___ 2.284
19 ___ 2.164
18 ___ 2.043
17 ___ 1.923
16 ___ 1.803
15 ___ 1.683
14 ___ 1.563
13 ___ 1.442
12 ___ 1.322
11 ___ 1.202
10 ___ 1.082
9 ___ 0.9616
8 ___ 0.8414
7 ___ 0.7212
6 ___ 0.6010
5 ___ 0.4808
4 ___ 0.3606
3 ___ 0.2404
2 ___ 0.1202
1 ___ 0.0000

20 ISOVALEURS

Iso M

Figure 12.

$M_\infty = 2$

$Re_\infty = 10\,000$

Version 2.04 de Portran 3d INRIA le 13:07:1989 a 11h 01mn. Utilisateur: boivin Dessin 1

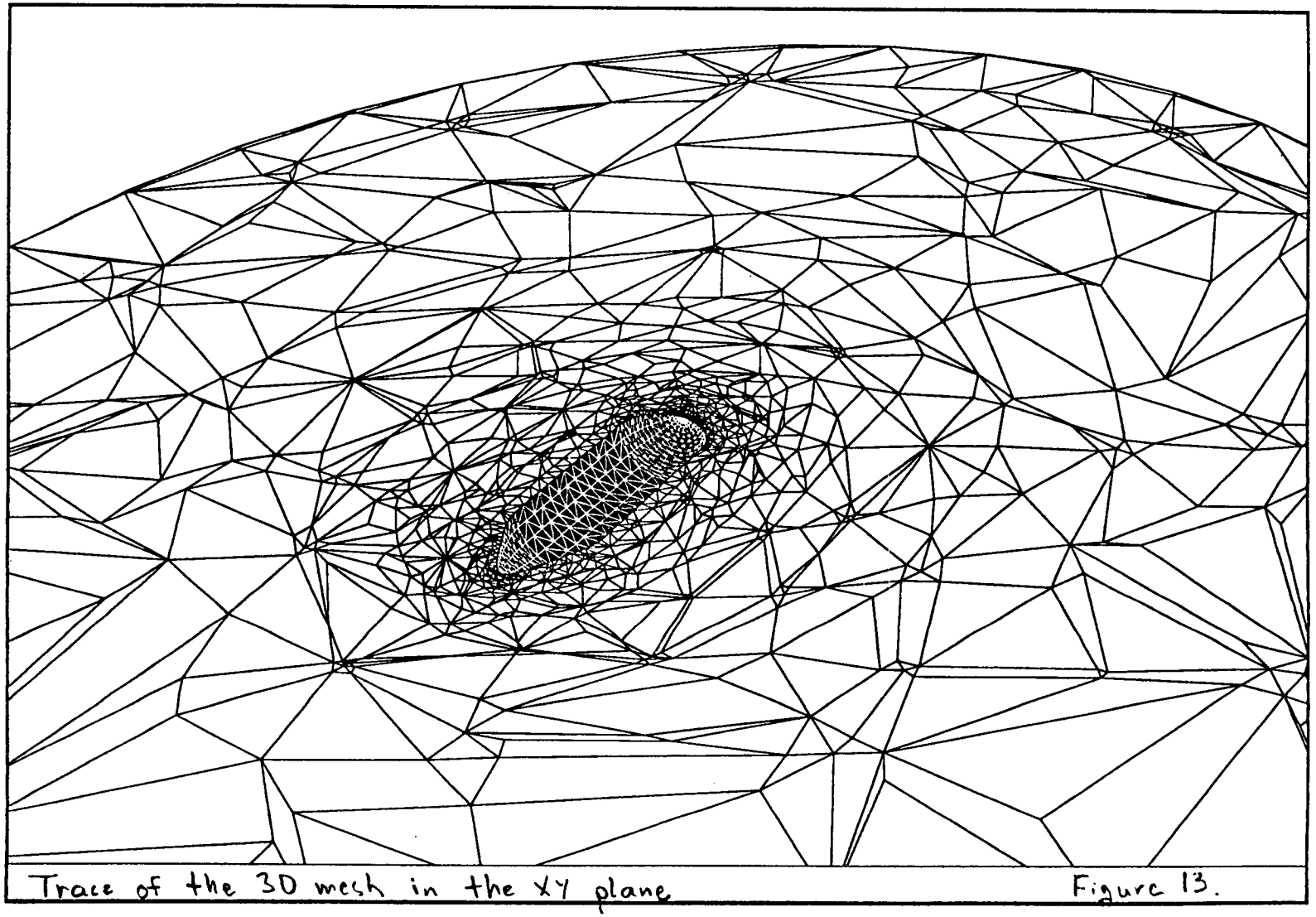

Trace of the 3D mesh in the XY plane. Figure 13.

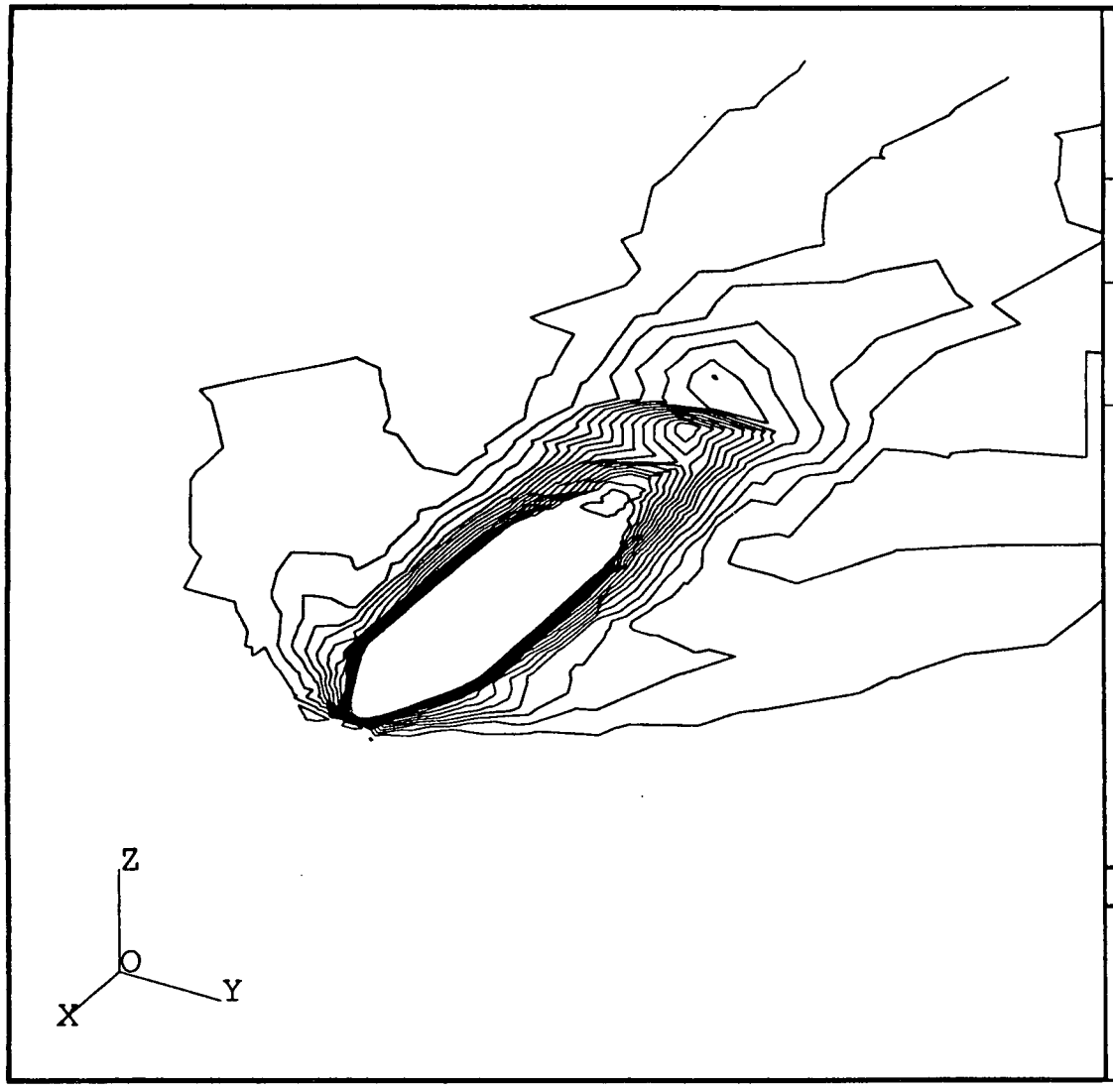

MODULEF : boivin

11/08/89
balle.mail
balle.coor
solu.b

3110 NOEUDS
29442 FACES
14023 TETRAEDRES

OBSERVATEUR SPHERIQUE :
30. 30. 8.0
OUVERTURE :
11.

ISOVALEURS : 20
INCONNUE : 1 MNEMO :VN

20	2.193
19	2.077
18	1.962
17	1.847
16	1.731
15	1.616
14	1.500
13	1.385
12	1.270
11	1.154
10	1.039
9	0.9233
8	0.8079
7	0.6925
6	0.5771
5	0.4616
4	0.3462
3	0.2308
2	0.1154
1	0.0000

PEAU VUE + ELIMINATION Figure 14.

$M_\infty = 2$

$Re_D = 5000$

Version 2.04 de Portran 3d LMHLA *le 11:08:1989 a 15h 17mn. Utilisateur: boivin Dessin 1*

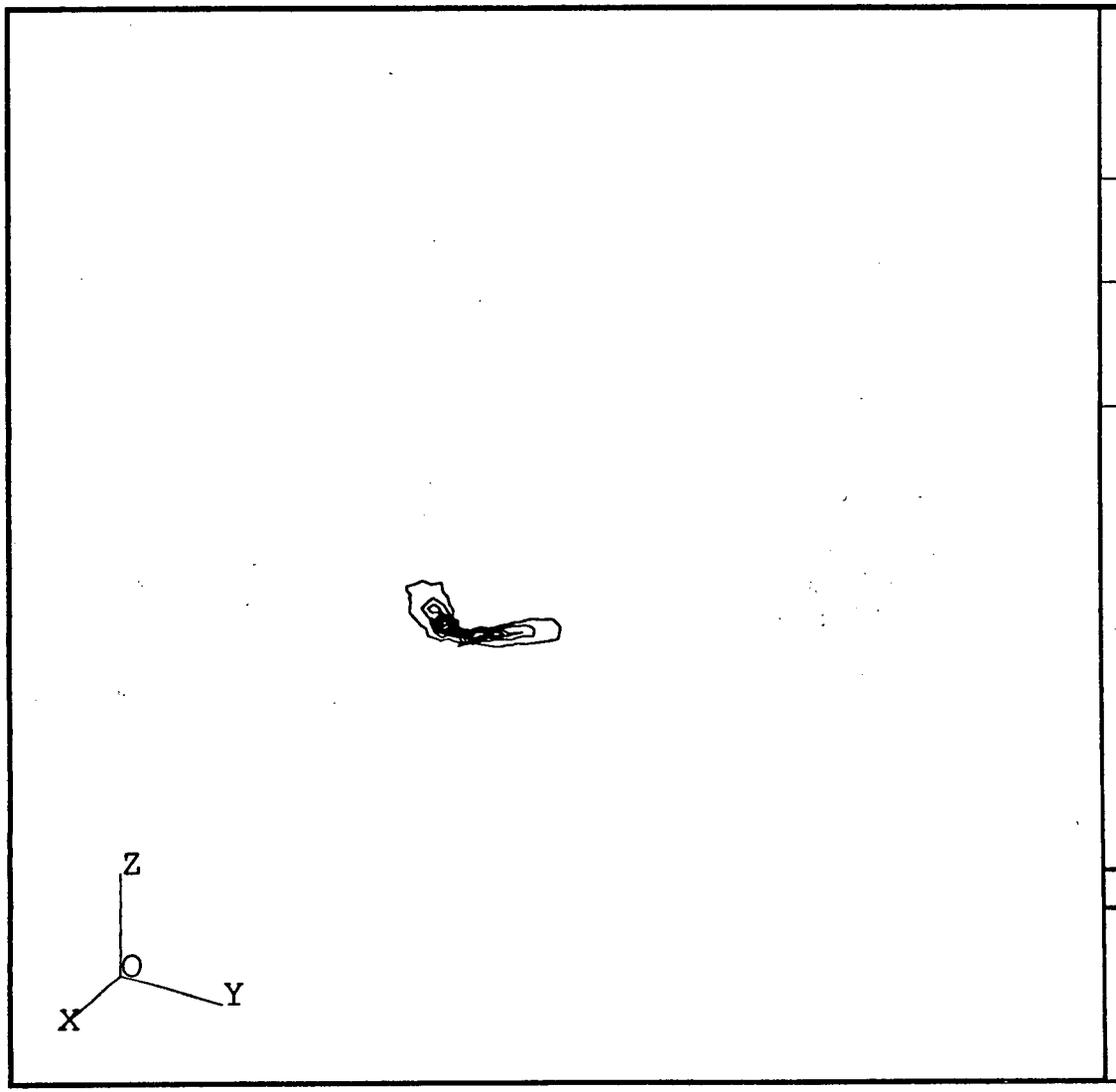

MODULEF : boivin

11/08/89
balle.mail
balle.coor
solu.b

3110 NOEUDS
29442 FACES
14023 TETRAEDRES

OBSERVATEUR SPHERIQUE :
30. 30. 16.
OUVERTURE :
11.

ISOVALEURS : 20
INCONNUE : 1 MNEMO :VN

20 0.3970
19 0.3761
18 0.3552
17 0.3343
16 0.3134
15 0.2925
14 0.2716
13 0.2507
12 0.2298
11 0.2089
10 0.1880
9 0.1671
8 0.1463
7 0.1254
6 0.1045
5 0.8357E-01
4 0.6268E-01
3 0.4179E-01
2 0.2089E-01
1 0.1602E-17

$|u|^6 |u \cdot \nabla u|$

PEAU VUE + ELIMINATION

Figure 15.

Criteria for the mesh enrichment preess

Version 2.04 de Perform 3d LMA/LA le 11/08/1989 a 16h 15mn. Utilisateur: boivin Dessin 1

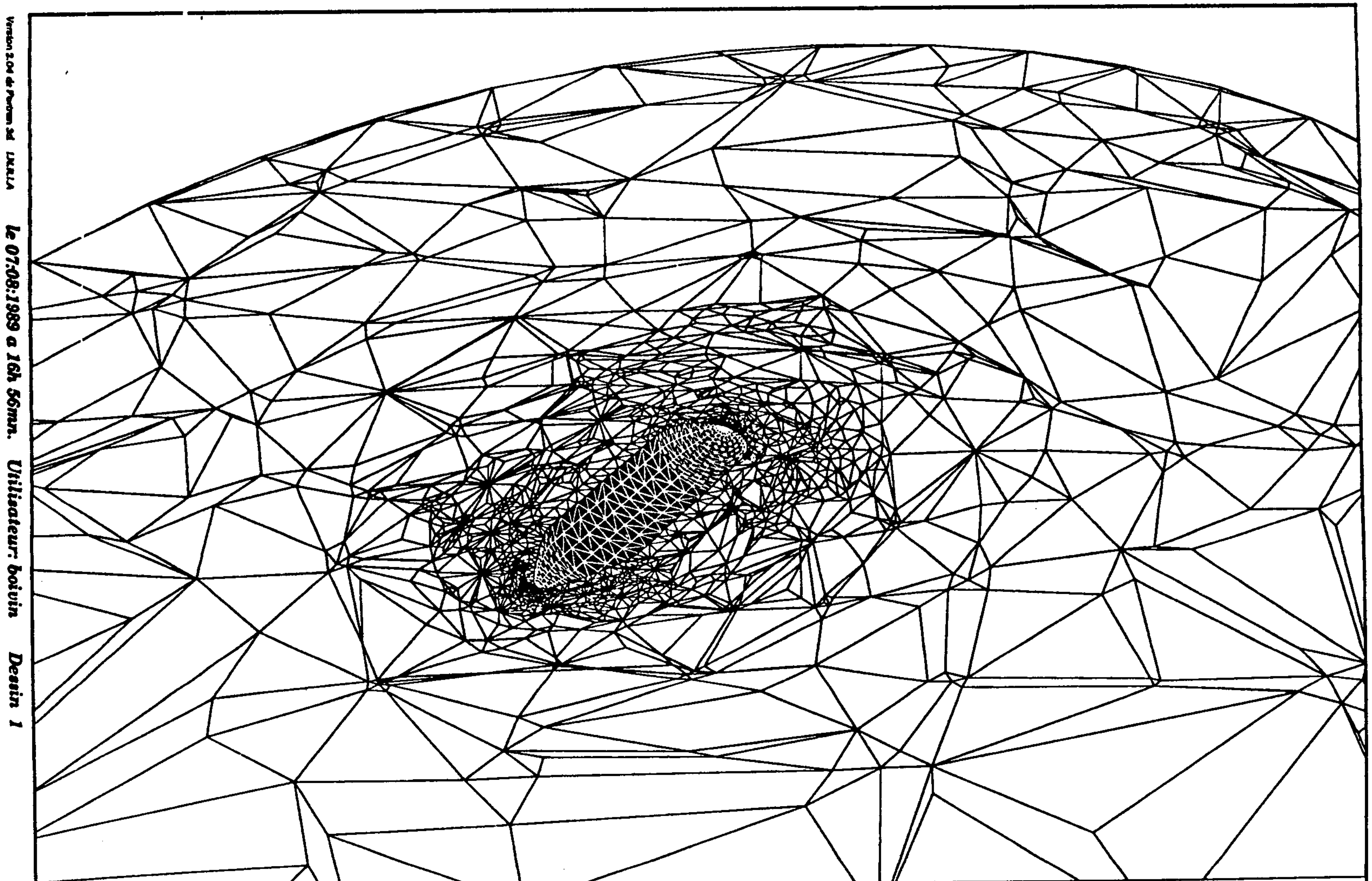

Trace of the 3D mesh in the XY plane Figure 16.

MODULEF : boivin

11/08/89
baller.mail
baller.coor
solu.b

6090 NOEUDS
56858 FACES
27731 TETRAEDRES

OBSERVATEUR SPHERIQUE :
30. 30. 8.0
OUVERTURE :
11.

ISOVALEURS : 20
INCONNUE : 1 MNEMO :VN

20	2.191
19	2.075
18	1.960
17	1.845
16	1.730
15	1.614
14	1.499
13	1.384
12	1.268
11	1.153
10	1.038
9	0.9224
8	0.8071
7	0.6918
6	0.5765
5	0.4612
4	0.3459
3	0.2306
2	0.1153
1	0.0000

Iso M

PEAU VUE + ELIMINATION Figure 17.

$M_{\infty} = 2$

$Re_{\infty} = 5000$

Version 2.04 de Perom 3d LNRIA **le 11:08:1989 a 15h 58mn. Utilisateur: boivin Dessin 1**

Imprimé en France
par
l'Institut National de Recherche en Informatique et en Automatique